Int J Clin Exp Med 2018;11(2):799-805
www.ijcem.com /ISSN:1940-5901/IJCEM0070101

Original Article

Effect of low frequency ultrasound plus fluorescent composite carrier in the diagnosis and treatment of methicillin-resistant staphylococcus aureus biofilm infection of bone joint implant

Huajun Zhou[1,2], Shiyuan Fang[2], Rong Kong[2], Weiwei Zhang[3], Kerong Wu[2], Rui Xia[2], Xifu Shang[2], Chen Zhu[2]

[1]Wannan Medical College, Wuhu City, Anhui Province, China; Departments of [2]Orthopedics, [3]Geriatrics, Anhui Provincial Hospital of Anhui Medical University, Hefei City, Anhui Province, China

Received November 30, 2017; Accepted December 28, 2017; Epub February 15, 2018; Published February 28, 2018

Abstract: Objective: To study the curative effect of low frequency ultrasound targeted radiation plus self-prepared human beta-defensins-3 (HBD-3) lipidosome microbubble fluorescent composite carrier for methicillin-resistant Staphylococcus aureus (MRSA) biofilm infection of intra-articular implant from an animal experiment based on the primary mechanism of the long-lasting recurrence of intra-articular implant infection (bacterial biofilm and bacterial internalization). Methods: Ti sheet and MRSA were co-cultivated for 24 hours. After the formation of biofilm, they were placed on both sides of dorsal spine of mice subcutaneously. These mice were divided into 6 groups (6 mice for each group) according to the form of carrier, which were HBD-3 group (Group A), HBD-3 fluorescent liposome group (Group B), HBD-3 lipidosome-microbubble fluorescent composite carrier group (Group C), low frequency ultrasound + HBD-3 group (Group D), low frequency ultrasound + HBD-3 fluorescent liposome group (Group E) and low frequency ultrasound + HBD-3 lipidosome-microbubble fluorescent composite carrier group (Group F). The remaining viable bacteria quantities in biofilm under different experimental treatment conditions were observed through coated sheet count, laser scanning confocal microscope and electron microscope. The relevant film-forming genes and drug resistant genes were analyzed quantitatively and statistically by real-time PCR. Results: Compared with other groups, the remaining viable bacteria percentage of Group F was significantly dropped, and the differences had statistical significance ($P<0.05$). The gene expression of Group F was higher than other groups, showing statistically significant differences ($P<0.05$). Conclusion: Low frequency ultrasound + HBD-3 lipidosome microbubble fluorescent composite carrier can greatly enhance the killing effect of HBD-3 to drug resistant staphylococcus in biofilm and inhibit the further maturity of bio-film. It also can help to treat MRSA biofilm infection in femoral implant of rats, thus providing a new thought for the current antibiotic treatment of bone and joint infection, and increasing the diagnosis rate and cure rate of implant infection at early stage in bone joint.

Keywords: Low-frequency ultrasound, fluorescent composite carrier, human beta-defensins-3, methicillin-resistant staphylococcus aureus biofilm infection

Introduction

Lipidosome, a vesicle with monolayer or multilayer film structure formed by the directional arrangement of phospholipid when dispersed in water, has the ability to envelop fat-soluble or water-soluble drugs. The antibiotic lipidosome prepared by using lipidosome as carrier has a good targeted bacterial biofilm effect, thus compensating the low concentration of hydrophilic antibiotic around the biofilm [1]. Moreover, lipidosome can also mediate the cell entry of antibiotics to realize intracellular anti-bacteria. Lipidosome is an effective sustained-release carrier as well. It can maintain high anti-microbial concentration for a long time and prevent internal drug from degradation [2, 3]. Low-frequency ultrasound usually refers to the frequency with 20 kHz to 1 MHz ultrasound. It has longer wavelength and can easilly pierce through the tissue. Low-frequency ultrasound combined with contrast agent has an important value in the treatment of tumors, and its biological effects include mechanical effects, cavi-

tation effects, thermal effects and chemical effects [4]. The cavatition created by low frequency ultrasound combined with microbubble contrast agent can enhance the permeability of the cell membrane and form some so-called "acoustic holes", so that the plasmid can enter the cell, and the gene transfection efficiency can be increased [5]. SonoVue, whose microbubble wall consists of phospholipid, is a commercialized microbubble contrast agent (MBCA) that contains sulfur hexafluoride gas. This FDA approved agent has been widely used in clinical ultrasound imaging. By binding specific ligands onto the surface of contrast agent, the imaging and targeted imaging of the lesion can be achieved at the molecular level, and the targeted treatment of drug can be mediated by load it with microbubble. An ideal microbubble possesses the ability to realize good targeted imaging and targeted treating, so as to increase the specificity and accuracy of diagnosis and treatment. The experiment of Joel E has shown that, the particle diameter of a microbubble with good imaging and cavitation effect should reach micron level. However, particles with this diameter cannot penetrate capillary wall, making it hard to carry drug into the lesion to take its effect [6]. It has been discovered in recent years that human beta-defensins-3 (HBD-3) is a new β-defensin endogenous antibiotic peptide with features like non-toxicity, broad spectrum and stable physical and chemical properties. It has strong bactericidal effects for gram-positive/negative bacteria and fungus, and can connect congenital and acquired immune responses through the mediation of Toll-like receptor [7]. The minimum inhibitory concentration (MIC) of HBD-3 against various gram positive bacteria is only 1.6-16 mg/L, and its MIC against staphylococcus aureus is slightly lower than vancomycin [8, 9]. So far, the *in vivo* application of antibacterial peptide HBD-3 in treating infections is faced with the biggest barrier--the degradation of polypeptide in the body. Gene transfection can help solving the degradation of HBD-3 and maintain a stable HBD-3 concentration in the body. Mannina et al. have proved that the tissue-engineered skin carrying target gene can continuously express HBD-3 and treat the mice with staphylococcus aureus infection in wound secondary to third-degree burns [4]. However, due to the high cost and hidden dangers of transgenic treatment, it is hard to apply it in clinical practice. Therefore, to find a new way to prevent the degradation of polypeptide and continuously keep it at a high concentration level has become a top priority. In this research, we carried out an animal experiment to explore the effect of low frequency ultrasound + fluorescent composite carrier for the diagnosis of MRSA biofilm infection in bone joint implant. Now the specific report is as follows.

Materials and methods

Experimental materials and instruments

Staphylococcus aureus ATCC6538 was purchased from American Type Culture Collection. The following materials were also bought: Ultrasonic contrast agent Microbubble SonoVue (Brzc-co); HBD-3 (Sigma Company); DSPE-PEG (Lipoid Company); anhydrous ethanol, glutaraldehyde and sodium dihydrogen phosphate (Xi'an Kehao Biological Engineering Co., Ltd.); donkey anti-mouse IgG antibody Cy3 label (Sigma Company); lysostaphin (Sigma Company); RNeasy mini kit (Qiagen Company); transmission electron microscope (TEM, Olympus Company), fluorescence microscope (Olympus), flow cytometry (Becton, Dickinson and Company), and US-100 physiotherapy and rehabilitation equipment (Ito Co., Ltd.).

The preparation of HBD-3 lipidosome-microbubble fluorescent composite carrier

HBD-3 was stored in the form of freeze-dried powder, diluted and dissolved in 0.1% acetic acid, and made into 1 mg/mL stock solution for storage. HBD-3 lipidosome was prepared with thin-film dispersion method and freeze-thawing method. A total of 15 mL 1.25% glutaraldehyde solution was mixed with 5 mL HBD-3 lipidosome for reaction. Rhodamine was used to mark lipidosome. After dialysis, 0.8 μm cellulose filter membrane was used for filtration. A total of 1 mg DSPE-PEG was added into 5 mL SonoVue microbubble suspension to obtain amino-microbubbles. And 1.5 μg biotin-labeled specific antibody was then added into every $1*10^7$ microbubbles. Incubation was performed on ice for 30 minutes, and then centrifugation, floating and washing were conducted. Then the glutaraldehyde-lipidosome suspension was added for reaction, and floating method was employed to wash the complex to obtain HBD-3 lipidosome-microbubble dual fluorescent posi-

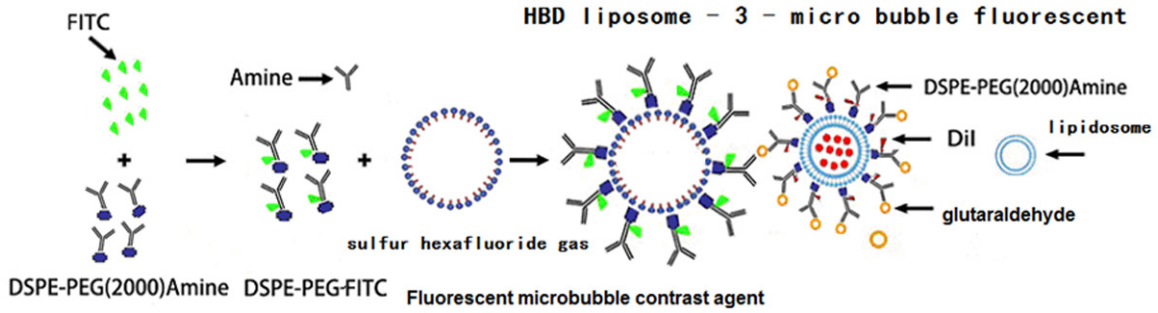

Figure 1. The structural diagram of HBD-3 lipidosome-microbubble fluorescent composite carrier HBD-3, human beta-defensins-3.

tively-labeled complex. See **Figure 1**. The encapsulation efficiency was calculated as per the lipidosome computation formula regulated in *Chinese pharmacopoeia 2010*. Five batches of sample were tested and measured for encapsulation efficiencies, when the efficiencies were higher than 80%, indicating a successfully encapsulation, the next step of experiment could then be conduct.

The treatment of biofilm and the preparation of model

The bacteria incubated overnight were diluted to 1:1,000, 50L ATCC43300 bacterial suspension (the bacterial count was around 106) was added into 0.5×BBL trypticase soy broth (TSBG, BD Biosciences) containing Ti sheet and 0.2% (w/v) glucose [9]. Before inoculation, the Ti sheet (1 mm thick, 10 mm in diameter) was sterilized and co-cultured with bacteria for 24 hours to form biofilm. Forty-eight BALB/c inbred male mice aged 8 to 12 weeks were randomly divided into 6 groups. After anesthesia through intraperitoneal injection, the back skin was cut opened to make an incision of about 10 mm under aseptic conditions. Following the formation of biofilm on the surface of Ti sheet, the Ti sheet was placed on the both sides of the back subcutaneously.

Experiential grouping and treatment methods

These mice were divided into 6 groups according to different carriers, 6 mice for each group: HBD-3 group (Group A), HBD-3 fluorescent lipidosome group (Group B), HBD-3 lipidosome-microbubble fluorescent composite carrier group (Group C), low frequency ultrasound + HBD-3 fluorescent group (Group D), low frequency ultrasound + HBD-3 fluorescent lipidosome group (Group E), and low frequency ultrasound + HBD-3 lipidosome-microbubble fluorescent composite carrier group (Group F). After injecting HBD-3 subcutaneously, ultrasound targeted microbubble or ultrasound was applied for 20 minutes locally, 3 times a day. A total of 30 μl contrast microbubble was injected subcutaneously around the Ti sheet. The ultrasonic frequency was maintained at 0.08 MHz with a sound intensity of 200 mW/cm^2 and 50% duty cycle. The mice in each group treated under different experiment conditions were executed before removing out the Ti sheet 7, 14 and 21 days after operation.

Bacterial count in biofilm on the surface of Ti sheet

In this experiment, the remaining viable bacteria inside biofilm were determined by the quantity of colony-forming units (CFUs) on Ti sheet surface. The Ti sheet was put into a disinfected sterile tube containing 0.5 mL 0.5×TSB, and the bacteria were collected by ultrasound bath shaking. Then a double dilution was conducted on TSA coated sheet, and a count analysis was performed 24 hours later. The result was the superficial area of bacterial count/Ti sheet material (CFU/mm^2).

Observation under laser scanning confocal microscope and scanning electron microscope

The experimental treatment conditions were the same with the above coated sheet counting method. The Ti sheets covered with biofilm were removed from the mice for fluorescent staining. There were two fluorescent staining solutions inside Live/Dead kit. Viable bacteria could display green fluorescence in SYTO fluorescent staining solution, while dead bacteria

Table 1. Count of viable bacteria on the carrier surface 7, 14 and 28 days after reaction by group ($\bar{x}$ ± sd, %)

Group	7 d	14 d	28 d
Group A	5.67±0.19	6.09±0.12	6.82±0.24
Group B	5.46±0.58	5.87±0.11	6.04±0.15
Group C	5.27±0.42	5.64±0.12	5.89±0.13
Group D	4.25±0.32	4.73±0.42	5.02±0.23
Group E	4.16±0.28	4.23±0.14	4.37±0.16
Group F	4.02±0.26	4.06±0.27	4.12±0.32
F	10.36	11.92	10.81
P	0.01	0.00	0.01

Note: Group A, HBD-3 group; Group B, HBD-3 fluorescent lipidosome group; Group C, HBD-3 lipidosome-microbubble fluorescent composite carrier group; Group D, low frequency ultrasound + HBD-3 group; Group E, low frequency ultrasound + HBD-3 fluorescent liposome group; Group F, low frequency ultrasound + HBD-3 lipidosome-microbubble fluorescent composite carrier group; HBD-3, human beta-defensins-3.

could display red fluorescence in PI. The morphological structure and bacterial viability of the biofilm on the surface of the Ti material were observed under laser scanning confocal microscope. Live and dead cells could be distinguished under fluorescent microscope. Viable bacteria would show green fluorescence due to the intact cell membrane, while dead bacteria would emit red fluorescence because of the damaged cell membrane. The Ti sheets covered with biofilm were removed out of the mice and fixed with 2.5% glutaraldehyde solution. Then it was dehydrated by using graded ethanol, dried at critical point and sprayed with metal. Finally, observation and photograph were taken under scanning electron microscope (SEM).

Real-time quantitative analysis

ATCC43300 was selected to analyze the expression of mecA gene. After removing the Ti sheets inside the mice, the bacterial biofilm on the surface of Ti sheet from each group was collected by ultrasound and sterile scraper, and then dissolved in bacteria RNA protective solution to protect the integrity of bacteria RNA. Then the solution was centrifuged in a centrifuge tube for 8 minutes at 4°C and 8,000 g; after discarding the protective solution, 200 L buffer solution of 100 g/mL lysostaphin was used to dissolve bacterial strain. Total RNA was extracted and reversely transcribed to cDNA. The gene primer sequence biosynthesized by Shanghai Sangon was applied for PCR amplification in the following conditions: 50°C, 20 seconds per cycle; 95°C, 15 seconds; 60°C, 1 minute, 40 cycles; 95°C, 10 minutes. 16S rRNA was used as the reference gene, and the CT value of each sample was considered the base. Each sample was repeatedly determined for three times on average.

Statistical treatment

The observation results were statistically processed with SPSS23.0 statistical software. The bacteria quantity was expressed as mean ± standard deviation ($\bar{x}$ ± sd). The comparison among multiple groups was performed by independent sample F test. P<0.05 was considered to indicate statistically significant difference.

Results

Count of viable bacteria on the carrier surface 7, 14 and 28 days after reaction by group

Compared with other groups, the viable bacteria percentage of Group F was apparently declined, and the differences had statistical significance (P<0.05). See **Table 1**.

The destructive effect on staphylococcus aureus and its biofilm in each group

Live/dead cells can be distinguished under fluorescence microscope. Live bacteria emit green fluorescence due to their intact cell membranes, while dead bacteria emit red fluorescence due to their damaged cell membranes. Compared with Group A, The quantity and density of red fluorescence and green fluorescence in Group F were reduced significantly, indicating a significant reduction of biofilm and bacteria after the intervention of ultrasound (**Figure 2**). After a further observation under SEM, there were still many small bacterial colonies on the surface of bacterial Ti sheets in Group A, Group B, Group C, Group D. On the contrary, only few small single colonies grew on the surface of Ti sheet in Group E or Group F. See **Figure 3**.

MecA gene expression in each group

The expression of mecA gene in Group F was higher than those in other groups, showing statistically significant differences (P<0.05). See **Table 2**.

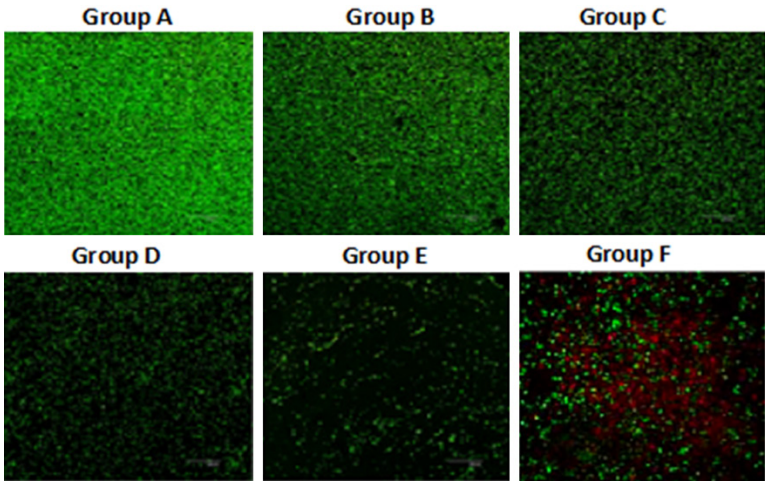

Figure 2. The destructive effect of different treatments on Staphylococcus aureus and its biofilm (200×). Group A, HBD-3 group; Group B, HBD-3 fluorescent lipidosome group; Group C, HBD-3 lipidosome-microbubble fluorescent composite carrier group; Group D, low frequency ultrasound + HBD-3 group; Group E, low frequency ultrasound + HBD-3 fluorescent liposome group; Group F, low frequency ultrasound + HBD-3 lipidosome-microbubble fluorescent composite carrier group; HBD-3, human beta-defensins-3.

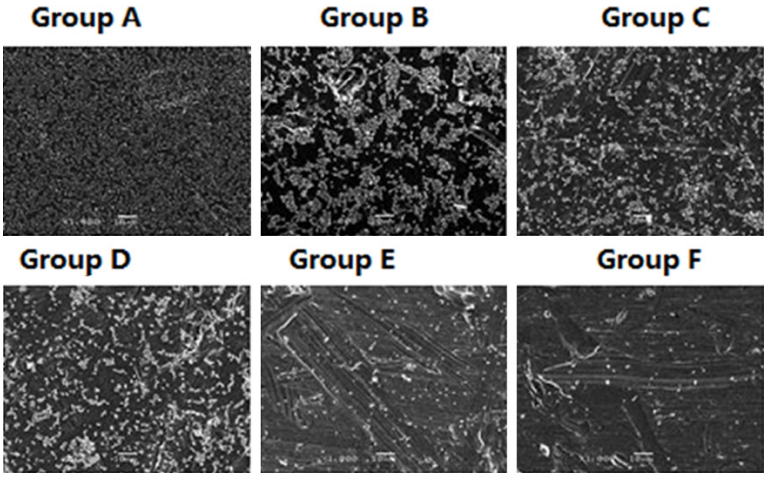

Figure 3. The formation of ATCC43300 biofilm on Ti sheet surface treated by different methods under SEM (1000×). Group A, HBD-3 group; Group B, HBD-3 fluorescent lipidosome group; Group C, HBD-3 lipidosome-microbubble fluorescent composite carrier group; Group D, low frequency ultrasound + HBD-3 group; Group E, low frequency ultrasound + HBD-3 fluorescent liposome group; Group F, low frequency ultrasound + HBD-3 lipidosome-microbubble fluorescent composite carrier group; HBD-3, human beta-defensins-3.

Discussion

First and foremost, by realizing the coupling of aminofluorescent with lipidosome, as well as testing the efficiency of carrying HBD-3 lipidosome by microbubble, taking lipidosome-microbble complex as the drug carrier in combination with targeted low frequency ultrasound can better improve the drug concentration of HBD-3 in the biofilm on the implant surface, which enhances the drug concentration in osteoblasts and has the effect of intracellular anti-infection [10, 11].

Secondly, by intercalating 1,2-distearoyl-sn-glycerol-3-phosphoethanol-amine-N-(Amino (polyethyl-eneglycol)-2000) (DSPE-PEG (2000) Amine) labeled with fluorescein isothiocyanate, the amino-SonoVue fluorescent microbubble is prepared [12, 13]. Eventually, the coupling between the fluorescent amino-microbubble and lipidosome can be achieved, and the efficiency of carrying HBD-3 lipidosome by microbubble can be tested [14]. This experimental study offers multi-functional characteristics to microbubbles while increasing the encapsulating capacity of drugs. The binding of the luminescent dye to microbubble lipidosome leads to the targeted imaging and targeted release of specific fluorescence of inflammatory sites. The present research aims to explore a better diagnosis and treatment method for common drug resistant biofilm infection in the arthrosis, and proposes to take the study of MRSA as an example to further study the application of HBD-3 and fluorescent composite carrier + targeted ultrasound in the diagnosis and treatment of other bacterial biofilm infections, such as gram negative bacteria, fungus, etc. [15-17].

In this experiment, we first prepared the nanoscale fluorescent HBD-3 lipidosome labeled with 1,1'-dioctadecyl-3,3,3',3'-tetramethylindocarbocyanine perchlorate, and studied the effect of low frequency ultrasound + fluorescent composite carrier in the diagnosis and treatment of MRSA biofilm infection in bone joint implant through in vitro and animal trials [18-20]. This study suggests that, the use of

Table 2. MecA gene (relative to 16S rRNA) expression value in each group

Group	MecA gene expression
Group A	198.72±28.06
Group B	182.18±26.38
Group C	180.25±40.26
Group D	126.12±14.26
Group E	105.02±13.26
Group F	85.83±2.31
F	15.08
P	0.00

Note: Group A, HBD-3 group; Group B, HBD-3 fluorescent lipidosome group; Group C, HBD-3 lipidosome-microbubble fluorescent composite carrier group; Group D, low frequency ultrasound + HBD-3 group; Group E, low frequency ultrasound + HBD-3 fluorescent liposome group; Group F, low frequency ultrasound + HBD-3 lipidosome-microbubble fluorescent composite carrier group; HBD-3, human beta-defensins-3.

low frequency ultrasound + HBD-3 lipidosome-microbubble fluorescent composite carrier can significantly enhance the killing effect of HBD-3 to MRSA in biofilm and inhibit the further maturity of bio-film. The mechanism of ultrasound-increased antibacterial effect of HBD-3 is complicated. On the one hand, as a mechanical pressure wave, ultrasound can generate high pressure and high shear force in the body, enhance the micro-convection between cells, increase the permeability of the cell membrane, and promote the passage of HBD-3 through the biofilm [16]. On the other hand, ultrasound can also increase the local temperature in ultrasound regions and generate free radicals in tissues, so as to potentially promote the permeability of bacterial cell membranes [17].

The formation of bacteria biofilm begin with the attachment of bacteria to host tissue or implant surface, and then the proliferation and aggregation of attached bacteria form biofilms. mecA gene coding for PBP2, which can reduce the antimicrobial activity of β-lactam antibiotics against pathogenic bacteria, is one of the mechanism for MRSA and methicillin-resistant Staphylococcus epidermidis (MRSE) to resist drug. Research shows that, ultrasound + HBD-3 liposome + microbubble can significantly lower the expression of MecA gene in biofilm, which may increase the sensitivity of MRSA and MRSE to oxacillin.

The indicators selected for the animal experiments in this study are still not comprehensive enough. It is expected that these indicators can be further enriched and improved in later studies.

In conclusion, ultrasound microbubble can increase the antimicrobial activity of HBD-3 against the biofilm formation of antibiotic-resistant bacteria and provide a non-invasive and targeted approach to treat antibiotic-resistant biofilm infections.

Acknowledgements

The present study was supported by the National Natural Science Foundation of China (Grant No. 81408185) the China Postdoctoral Science Foundation (Grant No. 2015M582900) and the Jiangsu Postdoctoral Science Foundation (Grant No. 1501146C).

Disclosure of conflict of interest

None.

Address correspondence to: Xifu Shang and Chen Zhu, Department of Orthopedics, Anhui Provincial Hospital of Anhui Medical University, No.9 Lujiang Road, Hefei 230001, Anhui Province, China. Tel: +86-0551-62283338; E-mail: shangxifudoc@126.com (XFS); zhuchenzcn@163.com (CZ)

References

[1] Krober M, Verwaaijen B, Wibberg D, Winkler A, Puhler A and Schluter A. Comparative transcriptome analysis of the biocontrol strain Bacillus amyloliquefaciens FZB42 as response to biofilm formation analyzed by RNA sequencing. J Biotechnol 2016; 231: 212-223.

[2] Kulshrestha S, Qayyum S and Khan AU. Antibiofilm efficacy of green synthesized graphene oxide-silver nanocomposite using Lagerstroemia speciosa floral extract: a comparative study on inhibition of gram-positive and gram-negative biofilms. Microb Pathog 2017; 103: 167-177.

[3] Liu MH, Li JK and Liu L. Perspectives on the related genes and detection methods of staphylococcus aureus biofilm formation. Food and Fermentation Industries 2016; 42: 265-269.

[4] Mannina G, Capodici M, Cosenza A, Cina P, Di Trapani D, Puglia AM and Ekama GA. Bacterial community structure and removal performanc-

es in IFAS-MBRs: a pilot plant case study. J Environ Manage 2017; 198: 122-131.
[5] Mallick I, Bhattacharyya C, Mukherji S, Dey D, Sarkar SC, Mukhopadhyay UK and Ghosh A. Effective rhizoinoculation and biofilm formation by arsenic immobilizing halophilic plant growth promoting bacteria (PGPB) isolated from mangrove rhizosphere: a step towards arsenic rhizoremediation. Sci Total Environ 2018; 610-611: 1239-1250.
[6] Kostka JE, Weston DJ, Glass JB, Lilleskov EA, Shaw AJ and Turetsky MR. The sphagnum microbiome: new insights from an ancient plant lineage. New Phytol 2016; 211: 57-64.
[7] Sadhasivam S, Palanivel S and Ghosh S. Synergistic antimicrobial activity of boswellia serrata roxb. ex colebr. (burseraceae) essential oil with various azoles against pathogens associated with skin, scalp and nail infections. Lett Appl Microbiol 2016; 63: 495-501.
[8] Rekha PD, Vasavi HS, Vipin C, Saptami K and Arun AB. A medicinal herb cassia alata attenuates quorum sensing in chromobacterium violaceum and pseudomonas aeruginosa. Lett Appl Microbiol 2017; 64: 231-238.
[9] Viszwapriya D, Subramenium GA, Radhika S and Pandian SK. Betulin inhibits cariogenic properties of streptococcus mutans by targeting vicRK and gtf genes. Antonie Van Leeuwenhoek 2017; 110: 153-165.
[10] Cui HY, Dai JM, Bai M, Zhou CQ, Tao GZ and Lin L. Lemongrass oil nanoliposomes against S. aureus biofilm formed on different materials. China Food Additives 2017; 55-60.
[11] Patil SV, Jayamohan NS and Kumudini BS. Strategic assessment of multiple plant growth promotion traits for shortlisting of fluorescent pseudomonas spp. and seed priming against ragi blast disease. Plant Growth Regulation 2016; 80: 47-58.
[12] Srinivasan R, Santhakumari S and Ravi AV. In vitro antibiofilm efficacy of piper betle against quorum sensing mediated biofilm formation of luminescent vibrio harveyi. Microb Pathog 2017; 110: 232-239.
[13] Salini R, Sindhulakshmi M, Poongothai T and Pandian SK. Inhibition of quorum sensing mediated biofilm development and virulence in uropathogens by Hyptis suaveolens. Antonie Van Leeuwenhoek 2015; 107: 1095-1106.
[14] Weng HF, Jiang TA, Wang Y, Zhao QY, and Ao JY. Construction methods and its efficiency of the delivery vehicle: complex of SonoVue conjugated to liposomes. Chinese Journal of Ultrasonography 2009; 18: 440-443.
[15] Raut JS and Karuppayil SM. Phytochemicals as inhibitors of candida biofilm. Curr Pharm Des 2016; 22: 4111-4134.
[16] Dutkiewicz J, Mackiewicz B, Lemieszek MK, Golec M and Milanowski J. Pantoea agglomerans: a mysterious bacterium of evil and good. Part IV. Beneficial effects. Ann Agric Environ Med 2016; 23: 206-222.
[17] Krober M, Verwaaijen B, Wibberg D, Winkler A, Puhler A and Schluter A. Comparative transcriptome analysis of the biocontrol strain bacillus amyloliquefaciens FZB42 as response to biofilm formation analyzed by RNA sequencing. J Biotechnol 2016; 231: 212-223.
[18] Li TT and Tang PF. Research progress on biofilm formation and regulation of staphylococcus aureus. Chinese Journal of Nosocomiology 2017; 27: 1673-1676.
[19] Rahman M. Bacillus spp. A promising biocontrol agent of root, foliar and postharvest diseases of plants. Bacilli and Agrobiotechnology 2017; 113-141.
[20] Sen T, Karmakar S and Sarkar R. Chapter 15-evaluation of natural products against biofilm-mediated bacterial resistance. Evidence-Based Validation of Herbal Medicine 2015; 14 Suppl 4: 321-338.